Proceedings of the ASME 2017 36th International Conference on Ocean, Offshore and Arctic Engineering
OMAE2017
June 25-30, 2017, Trondheim, Norway

OMAE2017-61468

PASSIVE CONTROL OF A PENTAPOD OFFSHORE WIND TUBINE UNDER EARTHQUAKES BY USING TUNED MASS DAMPER

Wenhua Wang
State Key Laboratory of Costal and Offshore Engineering
Faculty of Infrastructure Engineering
Dalian University of Technology
Dalian, China
Email: wang21106194@mail.dlut.edu.cn

Zhen Gao
Centre for Autonomous Marine Operations and Systems
Department of Marine Technology
Norwegian University of Science and Technology
Trondheim, Norway
Email: zhen.gao@ntnu.no

Xin Li
State Key Laboratory of Costal and Offshore Engineering
Faculty of Infrastructure Engineering
Dalian University of Technology
Dalian, China
Email: lixin@dlut.edu.cn

Torgeir Moan
Center for Ships and Ocean Structures
Department of Marine Technology
Norwegian University of Science and Technology
Trondheim, Norway
Email: torgeir.moan@ntnu.no

Bin Wang
Powerchina Huadong Engineering Corporation Limited
Hangzhou, China
Email: wangb@mail.dlut.edu.cn

ABSTRACT
The finite element model (FEM) of a pentapod offshore wind turbine (OWT) is established in the newly compiled FAST. The dynamic responses of the OWT are analyzed in detail. Further, a tuned mass damper as a passive control strategy is applied in order to reduce the OWT responses under seismic loads. The influence of the tuned mass damper (TMD) locations, mass and control frequencies on the reduction of OWT responses are investigated. A general configuration of TMD can effectively reduce the local and global responses to some degree, but due to the complexity of characteristics of the OWT structure and seismic waves, the single TMD can not obtain consistent controlling effects.

KEYWORDS: Offshore wind turbine, Finite element method, Earthquake analysis, TMD

1. INTRODUCTION
Initially the seismic analysis of onshore wind turbines are researched widely, such as the achievements of Prowell [1, 2], Asareh [3], Sadowski [4] and so on. Recently Katsanos [5] summarized the research performed by the scholars around the world, the developing of analysis methods are detailed introduced and the future research are enlightened in the paper. In recent research, Anastasopoulos [6], Kim [7] and Zheng [8] paid their attention to the responses of the fixed bottom OWT under seismic loads. Anastasopoulos [6] and Kim [7] discussed the nonlinearities of the foundation and substructure of the OWT under seismic loads by using FE method, Zheng [8] mainly focused on the interactions of seismic and wave loads for OWT under combined load cases.

The structural responses of the OWT show a significant variation under seismic loads, which may influence the safety of the structure. So the control of structural responses under extreme load conditions should be the key point in the OWT field, and the general passive structural control strategies such as tuned mass damper (TMD), multi tuned mass damper (MTMD), tuned liquid column damper (TLCD) can be considered. Fundamental theories of TMD and MTMD are introduced in detail in [9, 10], the mass and control frequency of the damper are proved to be the major parameters in optimal TMD design. Recently some scholars applied the TMD and MTMD in the research of vibration control of OWTs, e.g. Dinh [11], Stewart [12] and Lackner [13] investigated the behaviour of OWTs under operational loads in

consideration of TMD, and summarized the influence of TMD mass, amount and locations. Colwell [14] and Chen [15] validate the effects of TLCD on the OWT response by using numerical and experimental methods, respectively.

Initially the structural responses of a parked fixed bottom OWT under pure seismic loads are analyzed in the newly compiled FAST 8 [16]. The seismic analysis module is added in FAST 8 with the intention of perform dynamic analysis of fixed bottom OWT under combined seismic, wind and wave loads. Furthermore the passive control strategy of TMD is applied in the analysis in order to reduce the structural responses and protect the OWT from the seismic hazard. Different kinds of TMDs are applied in the investigation in order to find the proper control strategies under extreme load conditions. The control mechanisms and design standards of TMD are detailed introduced in Section 4.1.

2. FE MODEL OF PENTAPOD OWT

2.1. Structural Basic Parameters

An integrated OWT is developed based on the NREL 5MW baseline wind turbine [17] and a pentapod substructure of an actual OWT in China. Basic parameters of the NREL 5MW wind turbine are listed in Table 1, and Figure 1 shows the finite element model of the tower and substructure.

Table 1 Basic parameters of NREL 5MW wind turbine

Control	Variable speed, Collective pitch
Rotor, Hub diameter	126m, 3m
Hub height	90m
Cut in, Rated, Cut out Wind Speed	3m/s, 11.4m/s, 25m/s
Cut in, Rated Rotor Speed	6.9rpm, 12.1rpm
Rotor Mass	110,000kg
Nacelle Mass	240,000kg

Figure 1 Finite element model of the tower and Pentapod

2.2. Governing Equation under Combined Wind, Wave and Seismic Loads

The seismic loads analysis module is added in the recompiled FAST 8 in order to perform seismic analysis of OWT under combined load conditions. The motion of OWT under combined wind, wave and seismic loads can be expressed by Equation 1.

$$\mathbf{m}\ddot{\mathbf{u}}(t) + \mathbf{c}\dot{\mathbf{u}}(t) + \mathbf{k}\mathbf{u}(t) = \mathbf{f}_{wind}(t) + \mathbf{f}_{wave}(t) + \mathbf{f}_{seismic}(t) \quad (1)$$

where $\mathbf{m}$, $\mathbf{k}$ and $\mathbf{c}$ are the structural mass, stiffness and damping matrix, respectively; $\ddot{\mathbf{u}}$, $\dot{\mathbf{u}}$ and $\mathbf{u}$ are the vectors of structural acceleration, velocity and displacement, respectively; $\mathbf{f}_{wind}$, $\mathbf{f}_{wave}$ and $\mathbf{f}_{seismic}$ are the vectors of aerodynamic, hydrodynamic and seismic loads, respectively; $\ddot{\mathbf{u}}_g$, $\dot{\mathbf{u}}_g$ and $\mathbf{u}_g$ are the vectors of ground acceleration, velocity and displacement, respectively.

The aerodynamic and hydrodynamic loads are analyzed by the AeroDyn and HydroDyn modules in FAST 8 based on the coupled numerical model of the OWT.

Additional seismic module are added on the coupled numerical model in order to perform dynamic analysis of OWT under combined seismic, wind and wave loads. The expression of seismic loads in the module can be written as Equation 2 and 3.

$$f_{seismic}(t) = -m\ddot{u}_g(t) \quad (2)$$

$$f_{seismic}(t) = c\dot{u}_g(t) + ku_g(t) \quad (3)$$

where u_g, $\dot{u}_g$ and $\ddot{u}_g$ are the input vectors of ground displacements, velocities and accelerations, respectively.

Both the histories of displacement, velocity and acceleration can be applied in the horizontal and vertical directions in the seismic analysis. Moreover the seismic module can synthesize seismic excitations according to the provided responses spectrum.

In the study, the equivalent pile method is used to model the foundation of the OWT, and the bottom of the pile fixed on the seafloor directly.

2.3. Load Cases in Seismic Analysis

Firstly, the single seismic excitations are applied in the numerical analysis in order to research the responses of the fixed bottom OWT under earthquake loads. Table 2 lists the load cases and determined TMD control strategies proposed in the analysis. Figure 2 shows the time histories of the applied real recorded seismic excitations in the fore-aft (F-A) direction, such as El centro, Taft, North bridge and Chichi waves. These earthquake recordings are from the database of the Institute of Earthquake Engineering, Dalian University of Technology. Meanwhile, the Fourier amplitude of the seismic waves are showed in Figure 3. From the figures, the Chichi wave has the highest seismic intensity with the peak ground acceleration (PGA) 0.366g.

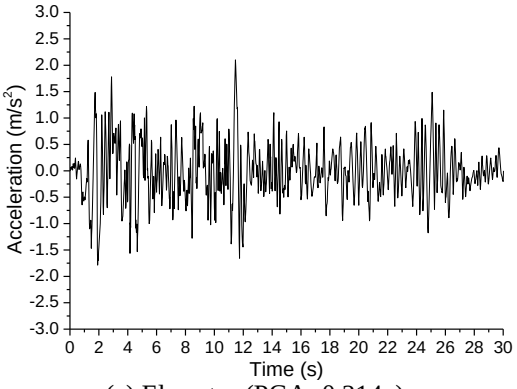

(a) El centro (PGA=0.214g)

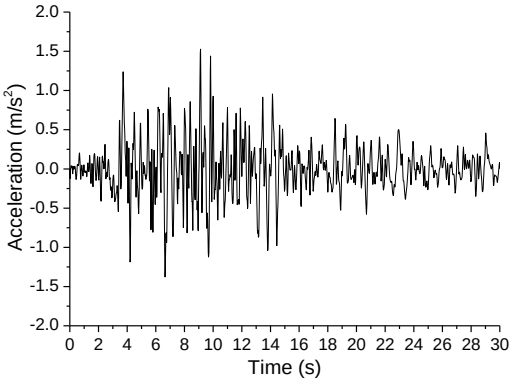

(b) Taft (PGA=0.155g)

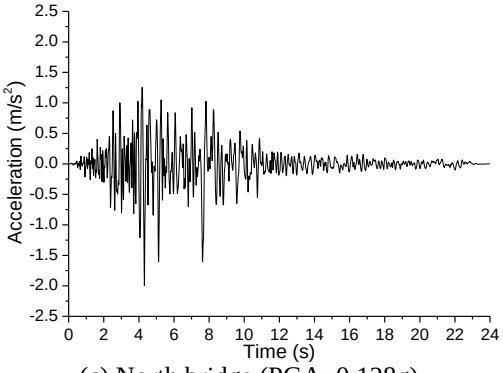

(c) North bridge (PGA=0.128g)

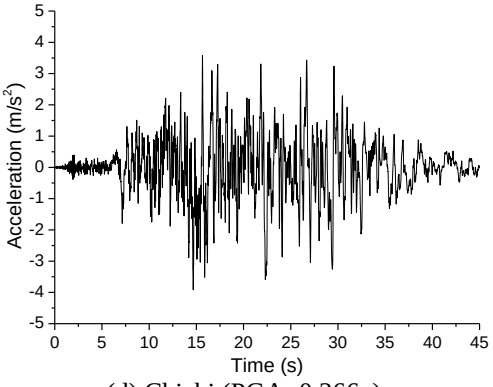

(d) Chichi (PGA=0.366g)

Figure 2 Time histories of seismic waves

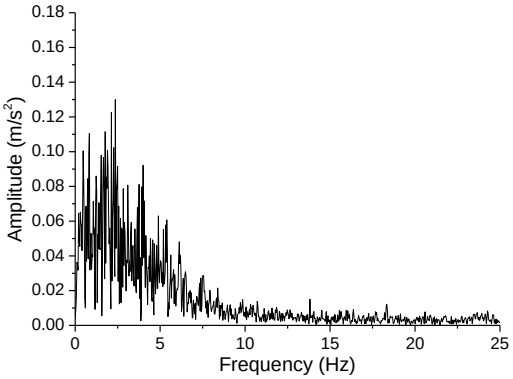

(a) El centro

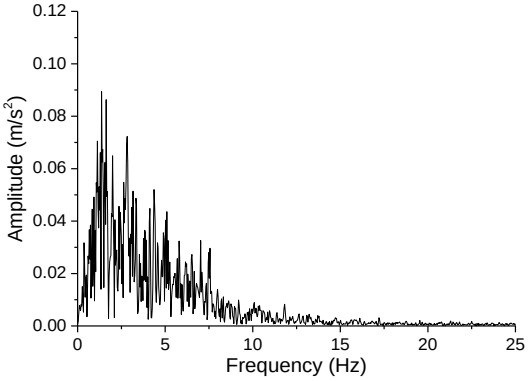

(b) Taft

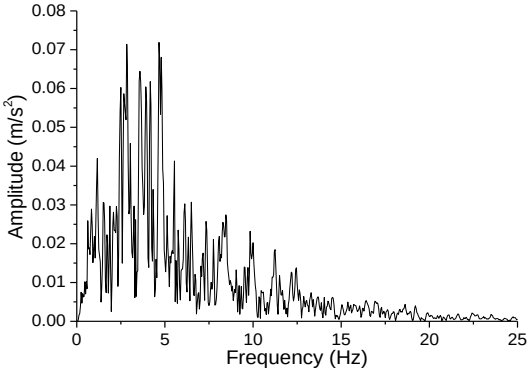

(c) North bridge

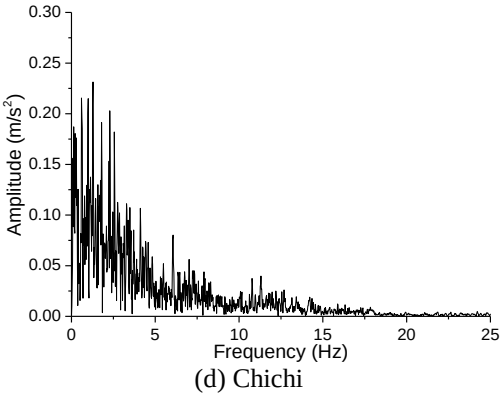

(d) Chichi

Figure 3 Fourier amplitude of seismic waves

Table 2 Load combinations for seismic analysis of a parked OWT in 23.45m water depth

Case No.	Seismic	Optimal TMD
E-0	El centro	Reference cases
T-0	Taft	
N-0	North bridge	
C-0	Chichi	
E-1	El centro	TMD 01
E-2		TMD 02
E-3		TMD 03
E-4		TMD 04
E-5		TMD 05
E-6		TMD 06
T-1	Taft	TMD 01
T-2		TMD 02
T-3		TMD 03
T-4		TMD 04
T-5		TMD 05
T-6		TMD 06
N-1	North bridge	TMD 01
N-2		TMD 02
N-3		TMD 03
N-4		TMD 04
N-5		TMD 05
N-6		TMD 06
C-1	Chichi	TMD 01
C-2		TMD 02
C-3		TMD 03
C-4		TMD 04
C-5		TMD 05
C-6		TMD 06

Both selected seismic excitations have abundant frequency components in the range of 0.1Hz-5Hz, which involves the lower fundamental frequencies of general offshore structures.

Basic parameters of the TMD are determined according to the optimal design standards, and the details of the optimal TMDs are listed in Table 5. The principle theories and optimal design standards of the TMD are introduced in detail in Section 4.

3. RESPONSES OF OWT UNDER SEISMIC LOADS

3.1. Dynamic Characteristics of OWT

The first two natural frequencies of OWT in F-A direction are 0.300Hz and 0,733Hz, Figure 4 shows the relevant mode shapes of the tower and substructure. The dash line represents the initial position of the OWT, and the solid is the deflected structure.

3.2. Structural Responses

3.2.1. Acceleration at the top of the tower

The OWT is in the parked s in the analysis. The total simulation time is 400s, and the seismic waves act on the structure at the time of 150s, Figure 5 shows the histories of acceleration at the tower top under the single seismic excitations. The dominant frequency components of the response are displayed in Figure 6. The 2nd structural frequency of 0.733Hz is found to be the dominant frequency of the acceleration at the tower top, but the 1st structural frequency can have comparable effect on the response under the Chichi wave which has a high seismic intensity, as shown in Figure 6(d).

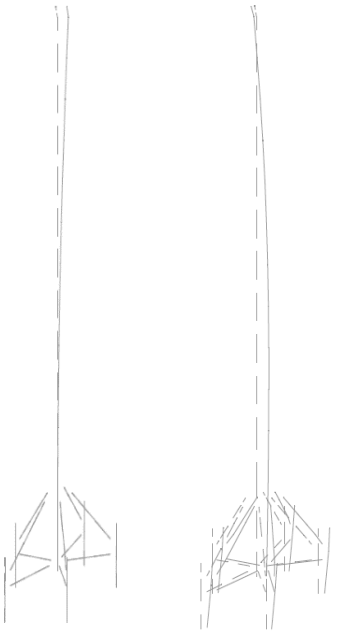

(a) 1st mode shape (b) 2nd mode shape

Figure 4 First two mode shapes of OWT in F-A direction

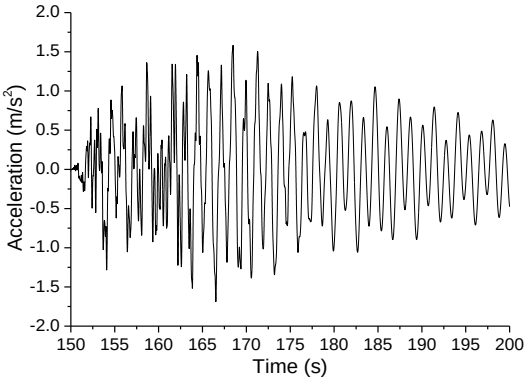

(a) El centro

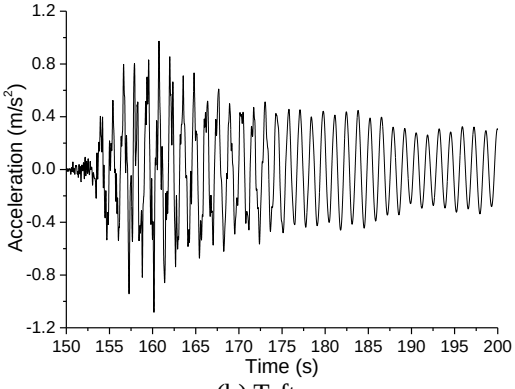

(b) Taft

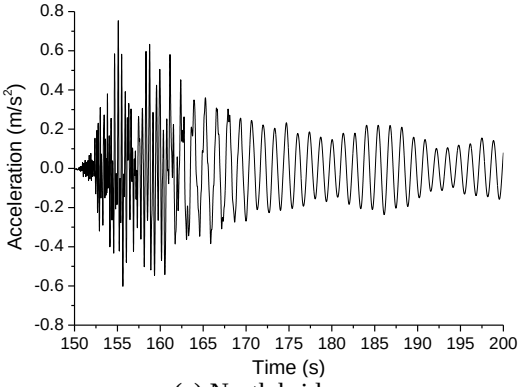

(c) North bridge

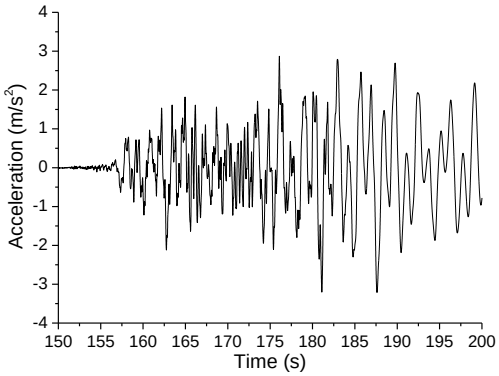

(d) Chichi

Figure 5 Tower top acceleration under pure seismic load

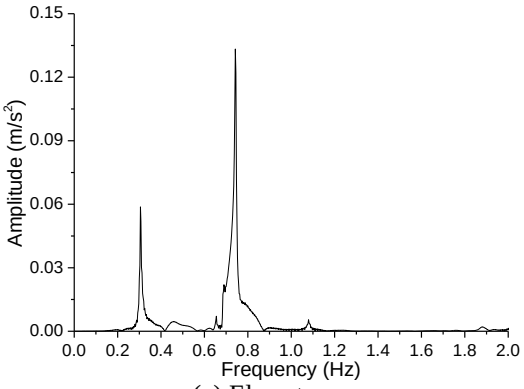

(a) El centro

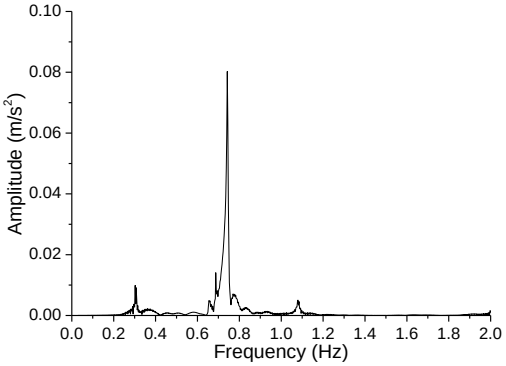

(b) Taft

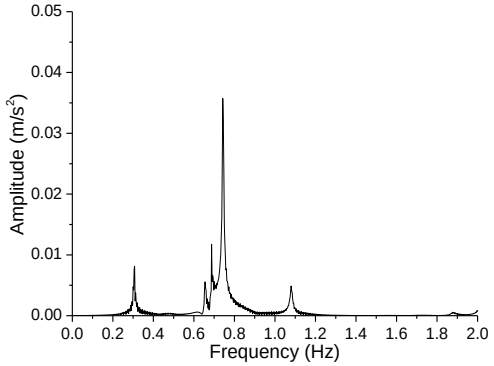

(c) North bridge

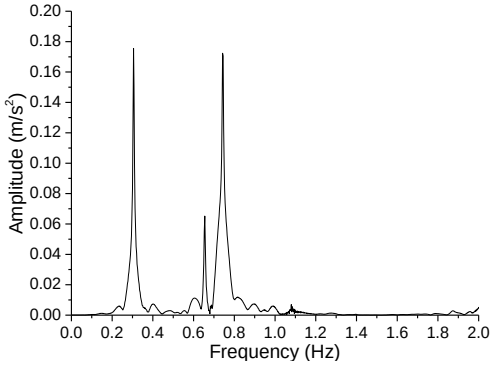

(d) Chichi

Figure 6 Fourier amplitude of tower top acceleration

Table 3 Statistics of the maximum acceleration at the tower top

Seismic wave	PGA (m/s^2)	Maximum value (m/s^2)	Minimum value (m/s^2)
El centro	2.101m/s^2	1.580	-1.685
Taft	1.527m/s^2	0.972	-1.081
North bridge	1.254m/s^2	0.753	-0.601
Chichi	3.587m/s^2	2.870	-3.213

Table 3 lists the statistics of the accelerations at the tower top under different seismic excitations. The Chichi wave stimulate maximum acceleration at the tower top due to its highest PGA. The accelerations at the tower top are so large under seismic excitations that can affect the operation of the mechanical system in the nacelle, such as the shaft, gearbox [18]. Thus, the acceleration of OWT at the tower top under seismic loads shall be reduced in order to ensure the operation of the OWT.

3.2.2. Maximum Accelerations along the Tower

Figure 7 shows the distribution of the normalized maximum tower accelerations along the tower. It can be found that the maximum tower accelerations are in the elevation range of 52.4m and 61.1m under the single seismic excitations. The amplifications of accelerations along the tower under seismic waves are almost same except those under the North bridge wave, while the amplifications of accelerations are nearly identical at the bottom and the top of the tower under the applied seismic

waves. Although the Chichi wave has the highest intensity, but it can't simulate highest tower accelerations, as shown in Figure 7, only the maximum responses under Taft wave are smaller than the Chichi wave.

Figure 8 shows the comparison of Fourier amplitudes of accelerations at the elevation of 8.73m and 52.4m under North bridge wave. From Figure 8, the first two mode shapes dominate the response of the OWT at the elevation of 8.73m, while the higher frequency components of 3.572Hz and 4.687Hz also have comparable effects on the tower acceleration at the elevation of 52.4m, which excited by the North bridge wave.

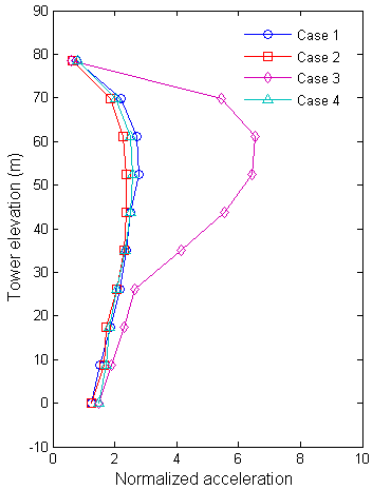

Figure 7 Maximum values of tower acceleration under pure seismic excitations

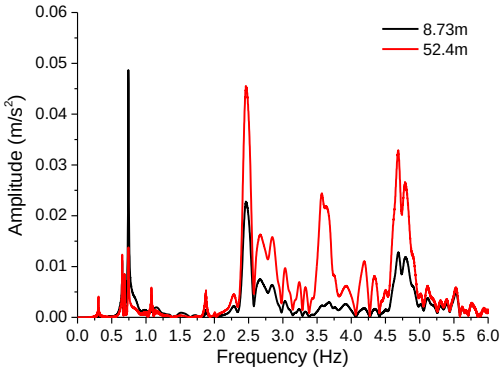

Figure 8 Fourier amplitude of maximum tower acceleration under North bridge seismic excitations

3.2.3. Responses of Base Shear and Bending Moment

The global response of base shear and bending moment at the bottom under pure seismic excitations are shown in Figures 9 and 10, respectively. The maximum and minimum of base shear and bending moment at the bottom are listed in Table 4. The global responses of base shear and bending moment are related to the PGAs of seismic excitations. The larger the PGAs are, the stronger the responses are. Meanwhile, the dynamic amplifications of the OWT are different under different seismic excitations due to spectral characteristics.

For the fixed bottom OWT, the global responses at the bottom are key parameters for structure safety assessment and optimization design. If the global responses under extreme load conditions are reduced to the allowable ranges by the application of proper structural control strategies, not only the operation stability but also the economy of the OWT will be improved significantly. Moreover, the fatigue life of OWT can also be extended due to the reducing of structural responses.

On the other hand, the structural responses of OWT under seismic loads are very different from the general buildings, so the effectiveness of the generalized control methods on the OWTs should be researched, such as the passive control strategy which applied widely in infrastructure engineering.

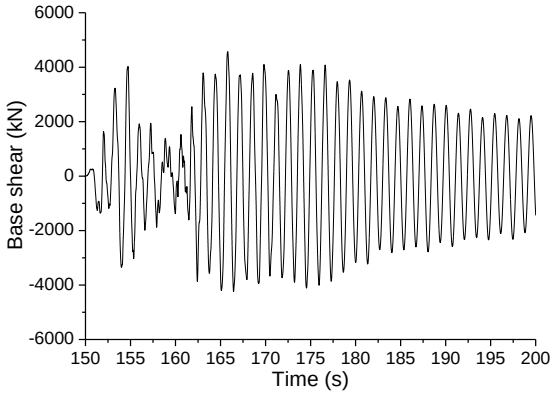

(a) El centro

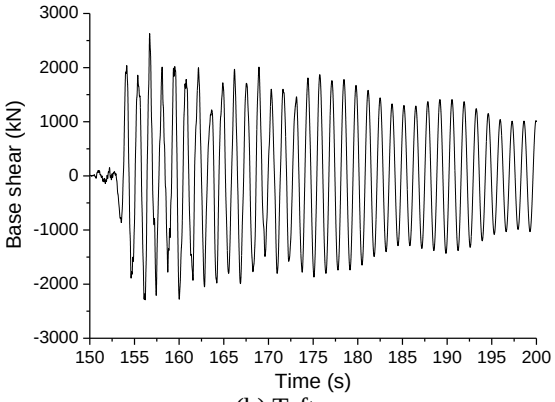

(b) Taft

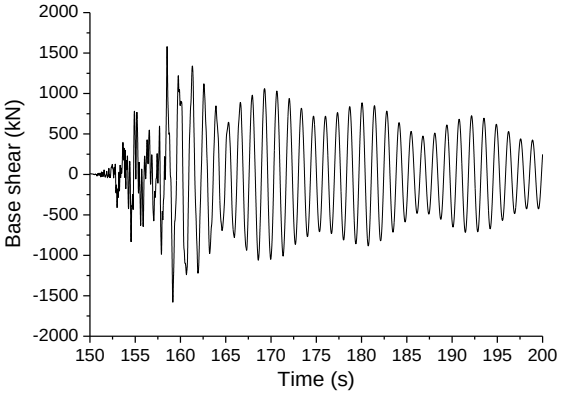

(c) North bridge

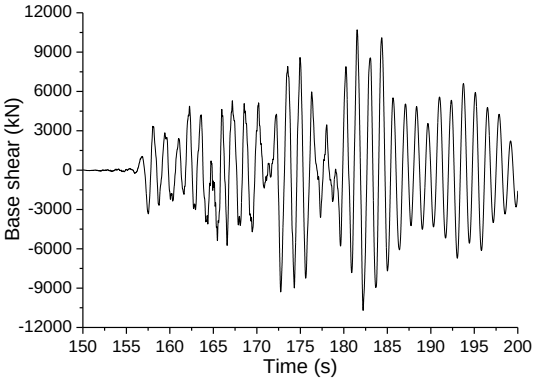

(d) Chichi

Figure 9 Global response of base shear

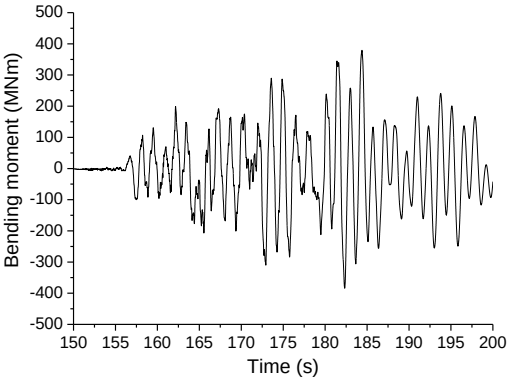

(d) Chichi

Figure 10 Global response of bending moment

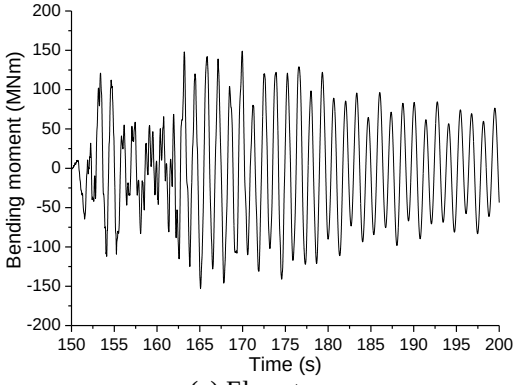

(a) El centro

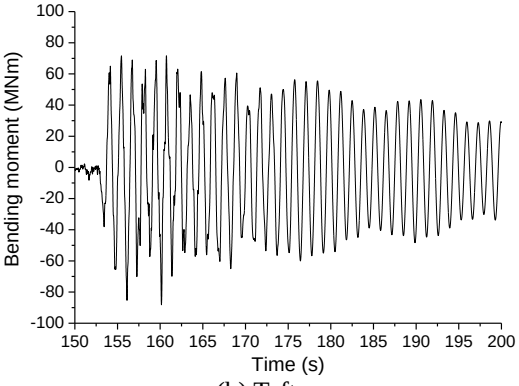

(b) Taft

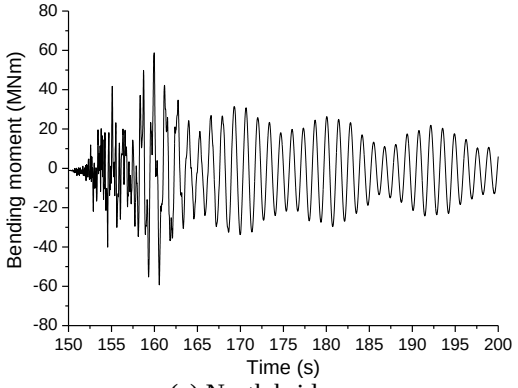

(c) North bridge

Table 4 Extreme values of base shear and bending moment

Case	Base shear (kN)		Bending moment (MN m)	
	Maximum	Minimum	Maximum	Minimum
El centro	4570	-4240	149	-153
Taft	2630	-2290	72	-88
North bridge	1580	-1580	59	-59
Chichi	10700	-10700	379	-384

4. PASSIVE CONTROL OF OWT

According to the introduction in Section 3, dynamic effects of OWT under seismic excitations is significant. The vibration control strategies such as TMD are necessary to control the structural responses and protect the OWT for the earthquakes.

4.1. Numerical Model of TMD

The Kane's dynamics is applied in FAST to derive the equations of motion, a detailed description about the relevant theories and governing equations can refer to [19, 20]. The TMD control method applied to OWT and embedded in FAST was presented in [13].

For a multi DOFs system, the equation of motion can be expressed in terms of Kane's theory.

$$F_i + F_i^* = 0 \left(i = 1, 2, \ldots, K\right) \tag{4}$$

where K is the amount of generalized DOFs; F_i is the generalized active forces; F_i^* is the generalized inertial forces.

The F_i and F_i^* can be expressed by using Equation 5 and 6.

$$F_i = \sum_{r=1}^{W} {}^{E}v_i^{X_r} \cdot F^{X_r} + {}^{E}\omega_i^{N_r} \cdot M^{N_r} \tag{5}$$

$$F_i^* = \sum_{r=1}^{W} {}^{E}v_i^{X_r} \cdot \left(-m_r\, {}^{E}a^{X_r}\right) + {}^{E}\omega_i^{N_r} \cdot \left(-{}^{E}\dot{H}^{N_r}\right) \tag{6}$$

where i is a index, i = 1, 2, …, *K*; W is the amount of substructures;

${}^{E}v_{i}^{X_r}$ and ${}^{E}\omega_{i}^{N_r}$ are the partial linear accelerations of center of mass (CM) point X_r and the partial angular velocities of substructure N_r in the inertial frame, respectively; F^{X_r} and M^{N_r} are the active forces and moments; m_r is the mass of substructure r; ${}^{E}a^{X_r}$ is the acceleration of the CM point of substructure r; ${}^{E}\dot{H}^{N_r}$ is the first time derivative of the angular momentum of substructure N_r.

According to the above Equations, the governing equations of TMD can be derived, detailed derivation are introduced in [21]. Equations 7 shows the governing equation of TMD in general form.

$$\ddot{\mathbf{r}}_{TMD} = \frac{1}{m}\mathbf{F}_{TMD} - \ddot{\mathbf{r}}_{P} - \boldsymbol{\omega}_{N} \times \left(\boldsymbol{\omega}_{N} \times \mathbf{r}_{TMD}\right) - \boldsymbol{\alpha}_{N} \times \mathbf{r}_{TMD} - 2\boldsymbol{\omega}_{N} \times \dot{\mathbf{r}}_{TMD} \quad (7)$$

where $\mathbf{r}_{TMD}$, $\dot{\mathbf{r}}_{TMD}$ and $\ddot{\mathbf{r}}_{TMD}$ are the vectors of TMD displacement, velocity and acceleration; m is the mass of TMD; $\mathbf{F}_{TMD}$ is the vector of external forces act on the TMD; $\boldsymbol{\omega}_{N}$ $\boldsymbol{\alpha}_{N}$ are the vectors of angular velocity and angular acceleration of the structural reference point.

The TMD is mainly consist of a mass, a spring and a damper. The excited forces on the TMD will act equal reactive force on the structure. Equations 8 and 9 are the derived reactive forces and moments of the TMD acting on the structure with respect to the local coordinate system of the nacelle of the OWT.

$$\vec{F}_{PG} = R_{N/G}^{T}\begin{bmatrix} k_X x_{TMD/PN} + c_X \dot{x}_{TMD/PN} - F_{ext_x} - F_{X_{TMD_Y/ON}} \\ k_Y Y_{TMD/PN} + c_Y \dot{Y}_{TMD/PN} - F_{ext_y} - F_{Y_{TMD_X/ON}} \\ -FZ_{TMDX/ON} - FZ_{TMDY/ON} \end{bmatrix} \quad (8)$$

$$\vec{M}_{PG} = R_{N/G}^{T}\begin{bmatrix} \left(-FZ_{TMDY/ON}\right) Y_{TMD/PN} \\ \left(FZ_{TMDX/ON}\right) x_{TMD/PN} \\ FX_{TMDY/ON} Y_{TMD/PN} \left(-FY_{TMDX/ON}\right) x_{TMD/PN} \end{bmatrix} \quad (9)$$

where $\vec{F}_{PG}$ and $\vec{M}_{PG}$ are the derived forces and moments of TMD; k_X and c_X are the stiffness and damping of the TMD; $x_{TMD/PN}$ and $\dot{x}_{TMD/PN}$ are the displacement and velocity of TMD in F-A direction in local coordinate system; $Y_{TMD/PN}$ and $\dot{Y}_{TMD/PN}$ are the displacement and velocity of TMD in S-S direction in local coordinate system; F_{extX} and F_{extY} are the external forces in F-A and S-S direction; $F_{Y_{TMD_X/ON}}$ and $FZ_{TMDX/ON}$ are the reaction forces of TMD arranged in F-A direction; $FX_{TMDY/ON}$ and $FZ_{TMDY/ON}$ are the reaction forces of TMD arranged in S-S direction.

The mass and location of TMD are key parameters for the vibration control, so different strategies of TMDs are proposed in the study in order to show the influence on the responses, as listed in Tabled 4. The arrangement of TMD in the nacelle of the OWT is shown in Figure 11. According to numerical analysis under seismic excitations, the first two mode shapes dominate the structural responses. So the first two fundamental frequencies are determined as the control frequency of TMD. The determination of the optimal TMDs is based on the optimal standards as expressed in Equation 15 and 16 [22, 23].

$$\mu = \frac{m_{TMD}}{m_{OWT}};\ f_{opt} = \frac{\omega_{TMD}}{\omega_{OWT}} \quad (10)$$

$$f_{opt} = \frac{(1 + 0.5\mu)^{\frac{1}{2}}}{(1 + \mu)} \quad (11)$$

$$\zeta_{opt} = 0.5\sqrt{\mu} \quad (12)$$

where μ and f_{opt} are the ratio of mass, frequency; f_{opt} and ζ_{opt} are the optimal frequency ratio and damping ratio; m_{TMD} and ω_{TMD} are the mass and radian frequency of TMD; m_{OWT} and ω_{OWT} are the mass and radian frequency of OWT.

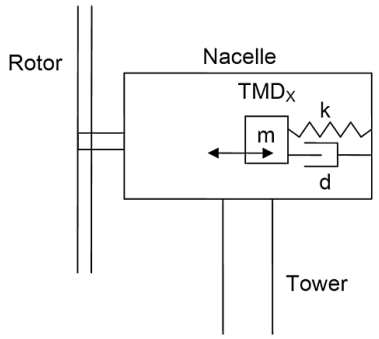

Figure 11 TMD located in the nacelle of OWT [13]

Table 5 Optimal parameters of TMD under seismic excitations

TMD No.	μ	m_{TMD} (kg)	f_{opt}	k_{TMD} (N/m)
01	1%	14897	0.993	52148
02	2%	29795	0.985	102769
03	3%	44692	0.978	151923
04	1%	14897	0.993	311315
05	2%	29795	0.985	613518
06	3%	44692	0.978	906962
TMD No.	ζ_{opt}	c_{TMD} (N/m/s)	Frequency (Hz)	Location
01	0.050	2787	0.300	Nacelle
02	0.071	7826	0.300	Nacelle
03	0.086	14272	0.300	Nacelle
04	0.050	6810	0.733	Tower base
05	0.071	19120	0.733	Tower base
06	0.086	34871	0.733	Tower base

4.2. Control Effect of Accelerations at the Tower Top

Figures 12 and 13 show the control effects of TMD on the accelerations at the tower top, and Figure 14 shows the relevant variation in the frequency domain. Moreover Tables 6-9 list the reduction of the statistics of tower accelerations under different seismic excitations, in which Δ is the percentage of the response reduction.

From Figure 12, the control effect of TMD can be divided into two phases. The first is the initial action of the TMD, such as the responses in 150s – 170s in Figure 12 (a), and the second is the continual action in the rest time of seismic excitation. In the first stage, only the damping result in controlling the acceleration at the tower top, thus, the control effect is insignificant. With the gradual activation of TMD, the inertial force of the TMD increases obviously in the second stage, so the responses of the structure decrease significantly under the combined inertial and damping forces.

Furthermore, it can be seen that the optimal TMD has more significant effects on the acceleration at the tower top from Figure 12 and 13, which can be attributed to the selection of the control frequencies of TMD. Based on the dynamic responses of the OWT, the control frequency of TMD is determined as 0.300Hz and 0.733Hz, namely, the first two fundamental frequencies of the OWT. The variation of Fourier amplitude of the acceleration at the tower top in Figure 14 also exhibits the control effect of TMD, which the amplitude of the second order frequency decrease significantly under the tower base TMD. On the other hand, the dominant frequency of the maximum tower acceleration is 2.467Hz which is beyond the control frequency of TMD. So the maximum tower acceleration can't show a significant reduction.

According to the statistics in Tables 6-9, it can be seen that the TMD 03 is the most effective control method for controlling the acceleration at the tower top under the El centro, North bridge and Chichi waves, while the damper of TMD 06 is the most effective under the Taft seismic excitation.

For the TMD 01-03, the damper is located at the top of tower with an increasing mass ratio. The reductions of responses under El centro, North bridge and Chichi seismic waves become more and more obvious with the increased TMD mass. For the Taft wave, the TMD arranged at the tower base is more effective than the TMD at the tower top, and the decreasing ratio can be as large as 29.03%. It also should be noted that although TMD installed on both the top and based of the tower can reduce the statistics of the accelerations at the tower top to some degree, but the above TMD layouts can not control the maximum acceleration of the tower effectively.

So arrange single TMD can not control the acceleration responses of the OWT comprehensively under seismic excitations, and the mass and locations of TMD are key parameters for the control effects.

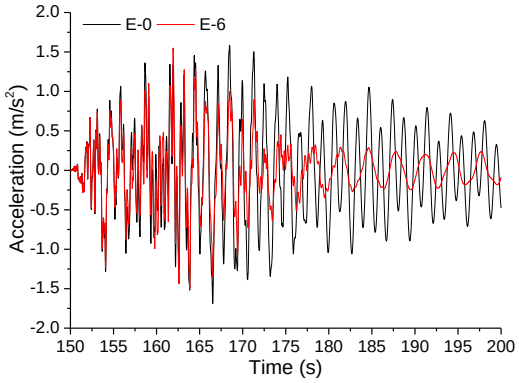

(a) El centro

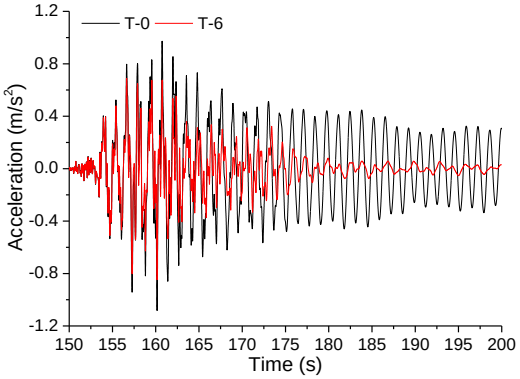

(b) Taft

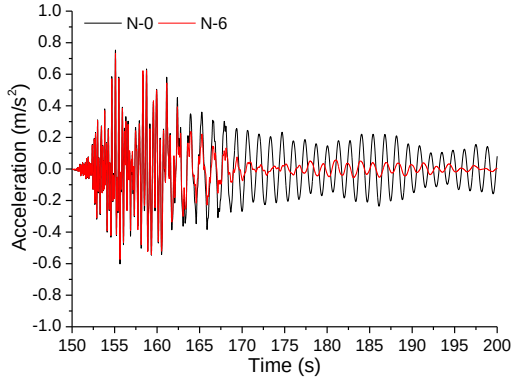

(c) North bridge

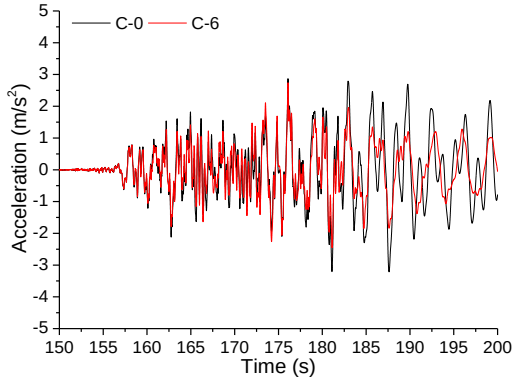

(d) Chichi

Figure 12 Control effects on tower top acceleration

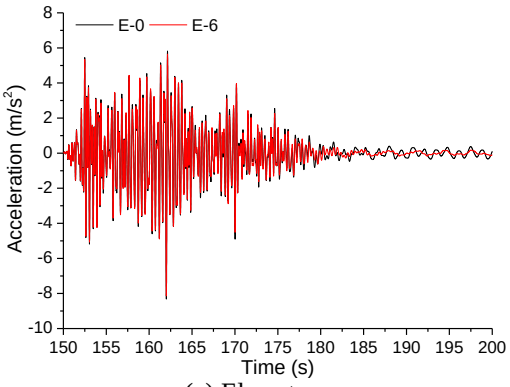

(a) El centro

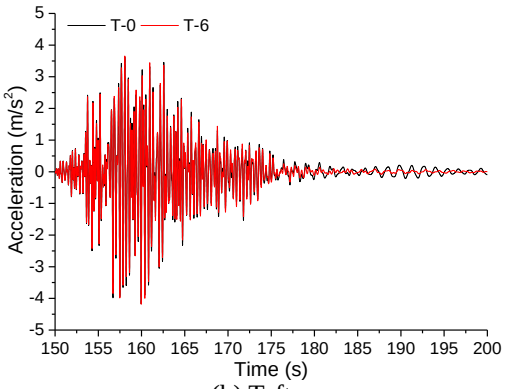

(b) Taft

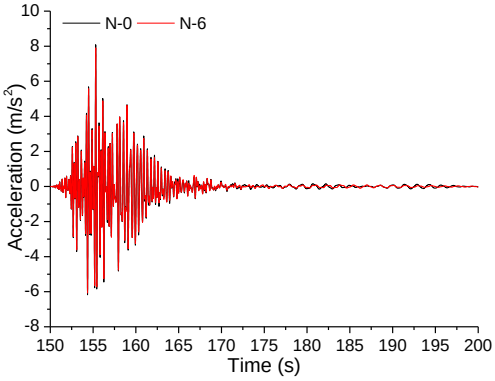

(c) North bridge

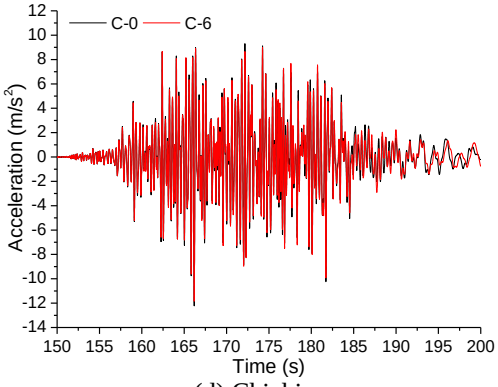

(d) Chichi

Figure 13 Control effects on maximum tower acceleration

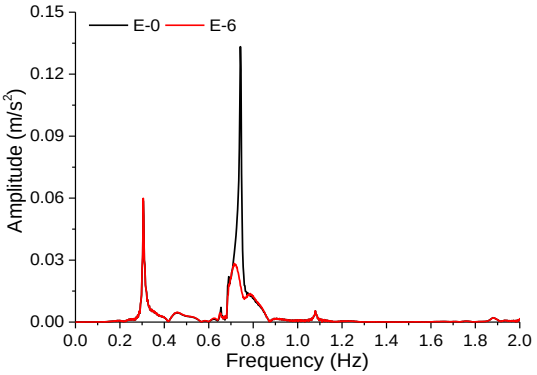

(a) El centro

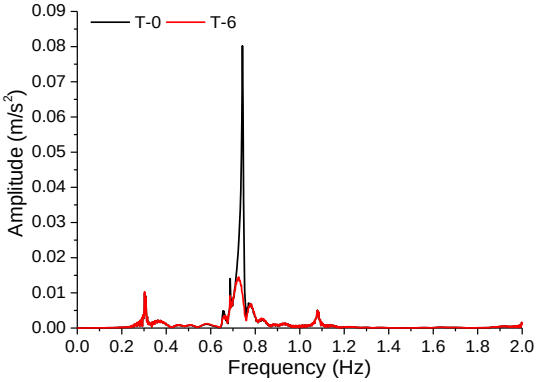

(b) Taft

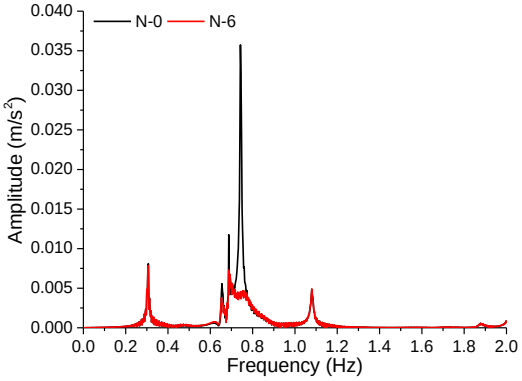

(c) North bridge

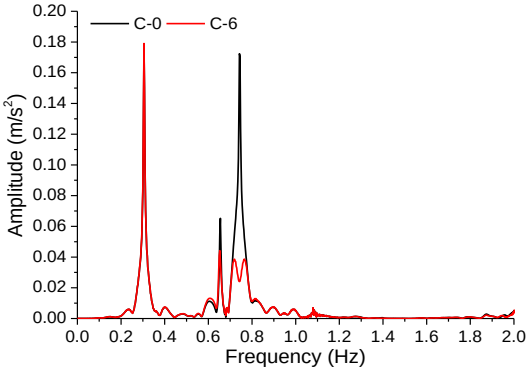

(d) Chichi

Figure 14 Control effects on tower top acceleration in the frequency domain

Table 6 Comparison of the tower accelerations (El centro)

Case No	Tower top acceleration (m/s^2)			
	Max	Δ (%)	Min	Δ (%)
5	1.537	2.72	-1.396	17.15
6	1.474	6.71	-1.424	15.49
7	1.404	11.14	-1.399	16.97
8	1.509	4.49	-1.567	7.00
9	1.547	2.09	-1.496	11.22
10	1.548	2.03	-1.497	11.16
Case No	Maximum tower acceleration (m/s^2)			
	Max	Δ (%)	Min	Δ (%)
5	5.696	2.05	-8.480	-1.94
6	5.653	2.79	-8.559	-2.88
7	5.642	2.98	-8.600	-3.38
8	5.704	1.91	-8.290	0.35
9	5.641	2.99	-8.138	2.18
10	5.641	2.99	-8.139	2.16

Table 7 Comparison of the tower accelerations (Taft)

Case No	Tower top acceleration (m/s^2)			
	Max	Δ (%)	Min	Δ (%)
11	0.944	2.88	-1.070	1.02
12	0.912	6.09	-1.049	2.96
13	0.880	9.43	-1.024	5.27
14	0.818	15.85	-0.963	10.96
15	0.732	24.62	-0.894	17.31
16	0.690	29.03	-0.847	21.68
Case No	Maximum tower acceleration (m/s^2)			
	Max	Δ (%)	Min	Δ (%)
11	3.619	-0.11	-4.187	-0.38
12	3.621	-0.17	-4.200	-0.70
13	3.621	-0.17	-4.211	-0.96
14	3.642	-0.75	-4.184	-0.31
15	3.651	-1.00	-4.187	-0.38
16	3.651	-1.00	-4.184	-0.31

Table 8 Comparison of the tower accelerations (North bridge)

Case No	Tower top acceleration (m/s^2)			
	Max	Δ (%)	Min	Δ (%)
17	0.723	3.91	-0.579	3.70
18	0.698	7.25	-0.555	7.56
19	0.674	10.39	-0.534	11.07
20	0.745	1.01	-0.590	1.73
21	0.739	1.83	-0.581	3.26
22	0.733	2.62	-0.573	4.68
Case No	Maximum tower acceleration (m/s^2)			
	Max	Δ (%)	Min	Δ (%)
17	8.078	0.00	-6.179	0.00
18	8.079	-0.01	-6.180	-0.02
19	8.079	-0.01	-6.180	-0.02
20	8.024	0.67	-6.144	0.57
21	7.966	1.39	-6.108	1.15
22	7.908	2.10	-6.071	1.75

Table 9 Comparison of the tower accelerations (Chichi)

Case No	Tower top acceleration (m/s^2)			
	Max	Δ (%)	Min	Δ (%)
23	2.807	2.20	-2.588	19.45
24	2.423	15.57	-2.121	33.99
25	2.141	25.40	-2.046	36.32
26	2.996	-4.39	-2.904	9.62
27	2.880	-0.35	-2.619	18.49
28	2.745	4.36	-2.447	23.84
Case No	Maximum tower acceleration (m/s^2)			
	Max	Δ (%)	Min	Δ (%)
23	9.272	0.19	-12.120	0.90
24	9.281	0.10	-12.070	1.31
25	9.417	-1.37	-12.040	1.55
26	9.207	0.89	-12.070	1.31
27	9.122	1.81	-11.950	2.29
28	9.000	3.12	-11.850	3.11

4.3. TMD Control of Base Shear and Bending Moment

Reduce the global responses of base shear and bending moment is another key point in the vibration control of the OWT. Figure 15 and 16 shows the control effects of TMD 06 on the base shear and bending moment, and Tables 10-13 list the reduction of the global responses on the base of different TMD strategies. According to the variation of time histories, the TMD 06 can reduce the global responses under El centro, Taft and North bridge effectively after the TMD is activated, as the response in the activated period (165s-200s) in Figure 15 (a). While the control effects are rather insignificant under Chichi wave, the time history shows an obvious reduction after 185s, which lag behind the activate time of the other seismic excitations. The larger PGA and more activated frequencies under high seismic intensity may limit the control effects of TMD under Chichi wave. For the base shear and bending moment, the TMD located at the tower base has better control effects than the TMD arranged at the tower top under El centro and Taft seismic waves based on the statistics in Tables 10 and 11. For the OWT under El centro wave, the TMD at the tower top may magnify the base shear to some degree. The single TMD barely has no effects on the global responses under North bridge seismic wave, and the TMD at the tower base even increase the base shear as the listed statistics in Table 12. According to Table 13, both the TMDs at the tower top and tower base can control the bending moment under Chichi wave, but the former is better. But the variation of base shear is more complex, such as TMD at the tower base can reduce the maximum value of the base shear effectively, but it also can amplify the minimum value.

So it is very hard to control the global responses comprehensively under different seismic excitations base on the previous introduction. Firstly, the determination of TMD locations, different locations has various effects on the global response. If the TMD arranged at an unsuitable place, it may can not reduce the response, but may magnify it. Another key parameter is the control frequency of the TMD, if the TMD involves the natural frequency of the OWT, it can achieve a better control effect with

a small mass ratio.

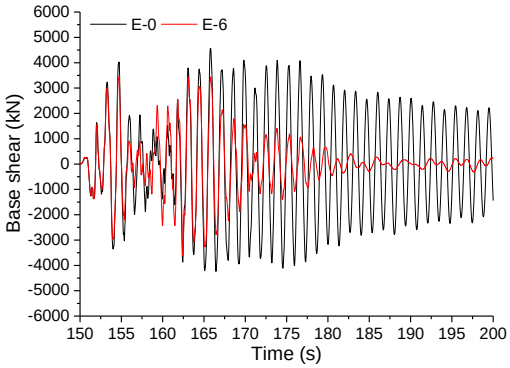

(a) El centro

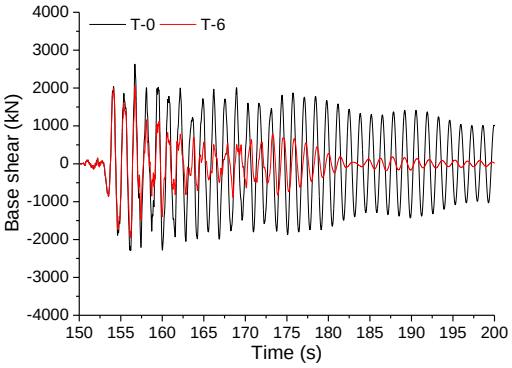

(b) Taft

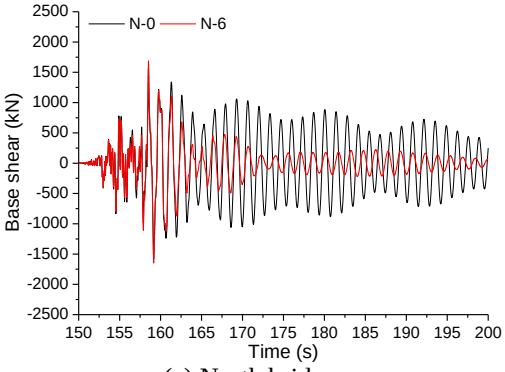

(c) North bridge

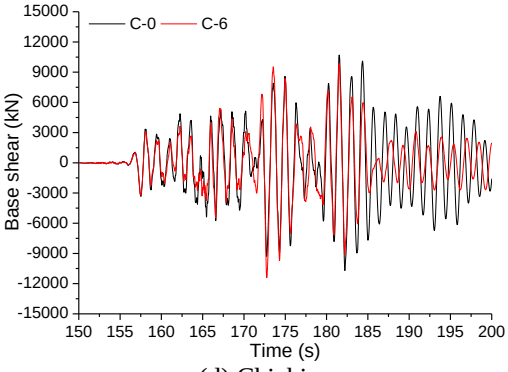

(d) Chichi

Figure 15 Control effects on base shear

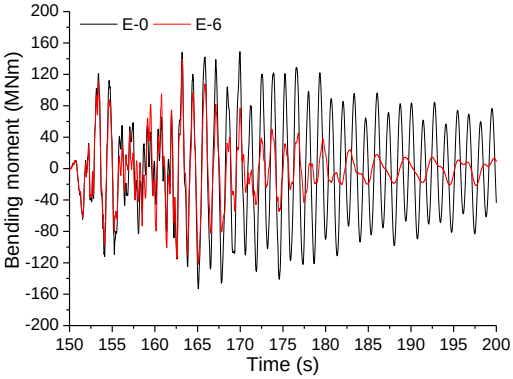

(a) El centro

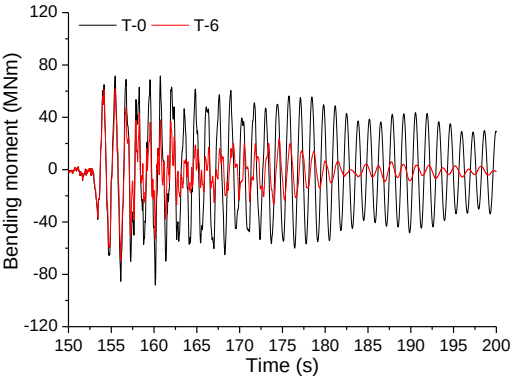

(b) Taft

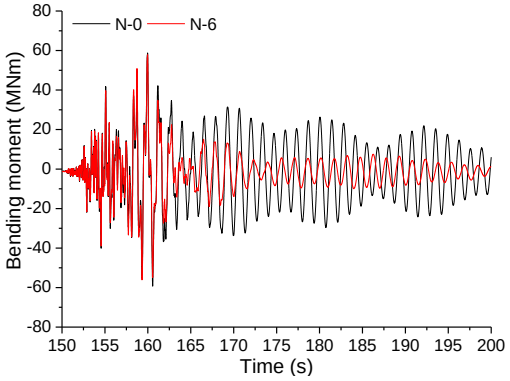

(c) North bridge

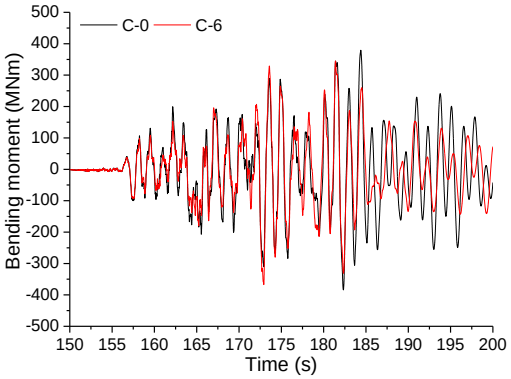

(d) Chichi

Figure 16 Control effects on bending moment

Table 10 Comparison of global responses (El centro)

Case No	Base shear (kN)			
	Max	Δ (%)	Min	Δ (%)
5	4700	-2.84	-4480	-5.66
6	4770	-4.38	-4560	-7.55
7	4820	-5.47	-4600	-8.49
8	4030	11.82	-3720	12.26
9	3450	24.51	-3620	14.62
10	3450	24.51	-3620	14.62
Case No	Bending moment (MN m)			
	Max	Δ (%)	Min	Δ (%)
5	143	4.03	-145	5.23
6	146	2.01	-149	2.61
7	148	0.67	-149	2.61
8	145	2.68	-132	13.73
9	142	4.70	-126	17.65
10	139	6.71	-122	20.26

Table 11 Comparison of global responses (Taft)

Case No	Base shear (kN)			
	Max	Δ (%)	Min	Δ (%)
11	2640	-0.38	-2300	-0.44
12	2650	-0.76	-2300	-0.44
13	2660	-1.14	-2310	-0.87
14	2390	9.13	-2150	6.11
15	2200	16.35	-2040	10.92
16	2040	22.43	-1950	14.85
Case No	Bending moment (MN m)			
	Max	Δ (%)	Min	Δ (%)
11	70	2.51	-86	2.84
12	71	0.98	-86	2.61
13	73	-1.39	-86	2.27
14	67	7.25	-77	12.37
15	64	10.74	-73	17.14
16	62	13.95	-69	21.34

Table 12 Comparison of global responses (North bridge)

Case No	Base shear (kN)			
	Max	Δ (%)	Min	Δ (%)
17	1580	0.00	-1580	0.00
18	1580	0.00	-1580	0.00
19	1570	0.63	-1580	0.00
20	1650	-4.43	-1640	-3.80
21	1680	-6.33	-1650	-4.43
22	1690	-6.96	-1650	-4.43
Case No	Bending moment (MN m)			
	Max	Δ (%)	Min	Δ (%)
17	59	0.34	-59	-0.17
18	59	0.34	-59	-0.17
19	59	0.51	-59	0.00
20	59	-1.02	-59	0.84
21	59	0.00	-57	3.88
22	58	1.53	-56	5.40

Table 13 Comparison of global responses (Chichi)

Case No	Base shear (kN)			
	Max	Δ (%)	Min	Δ (%)
23	10500	1.87	-10400	2.80
24	10200	4.67	-10400	2.80
25	10100	5.61	-10500	1.87
26	10400	2.80	-10800	-0.93
27	10000	6.54	-11300	-5.61
28	9860	7.85	-11400	-6.54
Case No	Bending moment (MN m)			
	Max	Δ (%)	Min	Δ (%)
23	314	17.15	-334	13.02
24	318	16.09	-327	14.84
25	318	16.09	-338	11.98
26	349	7.92	-352	8.33
27	349	7.92	-363	5.47
28	345	8.97	-367	4.43

5. CONCLUSION

This paper mainly discusses the structural responses of fixed bottom OWT under different seismic excitations and studies the control effects of single TMD on the reduction of structural responses. Furthermore, the effects of TMD's locations, mass and control frequency are studied. Following conclusions can be obtained based on the present research.

(1) Higher frequency components can be involved under seismic excitations, which can amplify the local structural responses, such as the accelerations along the tower.

(2) Nacelle is a suitable place to arrange TMD to reduce the acceleration at the tower top under seismic excitations, but for the maximum acceleration of the tower, the control effects are insignificant.

(3) The control effects of TMD on global responses of base shear and bending moment vary significantly under different seismic excitations. Sometimes an effective local control TMD may amplify the extreme values of the global responses.

(4) The location, mass and control frequency of the TMD are key parameters for controlling structural responses. The nacelle and tower base are the selective positions to arrange TMD. The control effects of the TMD can be obvious if it involves the dominated structural and seismic frequencies.

The present work mainly deal with the TMD control of OWTs under pure seismic excitations. The applicability of TMD under the combined seismic, wind and wave loads will be studied in future research. Furthermore, multiple tuned mass damper (MTMD) will be applied in the seismic analysis of OWT with the intention of reducing the structural responses comprehensively.

ACKNOWLEDGEMENT

This research was supported by the National Natural Science Foundation of China (Grant No. 51121005, 51609219) and the Open Fund Project of State Key Lab of Coastal and Offshore Engineering in Dalian University of Technology (No. LP1611). The Chinese Scholarship Council and the Department of Marine Technology (NTNU) are acknowledged to support this research.

REFERENCES

[1] Prowell, I., Elgamal, A., Uang, C. M., Enrique Luco, J., Romanowitz, H., Duggan, E. (2014). Shake table testing and numerical simulation of a utility scale wind turbine including operational effects. Wind Energy, 17(7), 997-1016. DOI: 10.1002/we.1615

[2] Prowell, I. (2011). An experimental and numerical study of wind turbine seismic behavior. PhD dissertation, University of California, San Diego.

[3] Asareh, M. A. (2015). Dynamic behavior of operational wind turbines considering aerodynamic and seismic load interaction. PhD dissertation, Missouri University of Science and Technology, Rolla.

[4] Sadowski, A. J., Camara, A., Málaga-Chuquitaype, C., Dai, K. (2016). Seismic analysis of a tall metal wind turbine support tower with realistic geometric imperfections. Earthquake Engineering & Structural Dynamics. DOI: 10.1002/eqe.2785

[5] Katsanos, E. I., Thöns, S., Georgakis, C. T. (2016). Wind turbines and seismic hazard: a state of the art review. Wind Energy. DOI: 10.1002/we.1968

[6] Anastasopoulos, I., Theofilou, M. (2016). Hybrid foundation for offshore wind turbines: Environmental and seismic loading. Soil Dynamics and Earthquake Engineering, 80, 192-209.

[7] Kim, D. H., Lee, S. G., Lee, I. K. (2014). Seismic fragility analysis of 5 MW offshore wind turbine. Renewable energy, 65, 250-256.

[8] Zheng, X. Y., Li, H., Rong, W., Li, W. (2015). Joint earthquake and wave action on the monopile wind turbine foundation: An experimental study. Marine Structures, 44, 125-141.

[9] Connor, J. J. (2003).Introduction to structural motion control. Prentice Hall.

[10] Zhou, F. L. (1997). Motion control of engineering structures (Chinese). Seismological Press.

[11] Dinh, V. N., Basu, B. (2015). Passive control of floating offshore wind turbine nacelle and spar vibrations by multiple tuned mass dampers. Structural Control and Health Monitoring, 22(1), 152-176.

[12] Stewart, G., Lackner, M. (2013). Offshore wind turbine load reduction employing optimal passive tuned mass damping systems. IEEE Transactions on Control Systems Technology, 21(4), 1090-1104.

[13] Lackner, M. A., Rotea, M. A. (2011). Passive structural control of offshore wind turbines. Wind energy,14(3), 373-388. DOI: 10.1002/we.426

[14] Colwell, S., Basu, B. (2009). Tuned liquid column dampers in offshore wind turbines for structural control. Engineering Structures,31(2), 358-368.

[15] Chen, J., Liu, Y., Bai, X. (2015). Shaking table test and numerical analysis of offshore wind turbine tower systems controlled by TLCD. Earthquake Engineering and Engineering Vibration,14(1), 55-75.

[16] Jonkman, J. M., Buhl Jr, M. L. (2005). FAST user's guide. National Renewable Energy Laboratory, Golden. Technical Report No. NREL/EL-500-38230.

[17] Jonkman, J., Butterfield, S., Musial, W., Scott, G. (2009). Definition of a 5-MW reference wind turbine for offshore system development. National Renewable Energy Laboratory, Golden. Technical Report No. NREL/TP-500-38060.

[18] Nejad, A. R., Guo, Y., Gao, Z., Moan, T. (2015). Development of a 5 MW reference gearbox for offshore wind turbines. Wind Energy, 19, 1089-1106.

[19] Kane, T., Levinson D. (1985). Dynamics: Theory and Applications. McGraw-Hill Inc.: East Roseville.

[20] Jonkman, J. (2007). Dynamics modeling and loads analysis of an offshore floating wind turbine. National Renewable Energy Laboratory, Golden. Technical Report No. NREL/TP-500-41958.

[21] Cava, L. W., Lackner, M. A. (2015). Theory manual for the tuned mass damper module in FAST v8. Technical Report. University of Massachusetts, Amherst. DOI: 10.1314/rg.2.1.4565. 9684.

[22] Connor, J. J. (2003).Introduction to structural motion control. Prentice Hall.

[23] Zhou, F. L. (1997). Motion control of engineering structures (Chinese). Seismological Press.